NUEMERICAL MODELLING AND EXPERIMENTAL STUDY OF MICROSTRIP- COUPLED RECTANGULAR DIELECTRIC RESONATOR ANTENNA

M. H. Neshati[1] and Z. Wu[2]

1- Electrical Dept. Sistan & Baluchistan University. Zahedan, 98164, Iran.
e-mail: neshat@hamoon.usb.ac.ir

2- Department of Electrical Engineering & Electronics,
University of Manchester Institute of Science & Technology,
Manchester M60 1QD, UK.
e-mail: z.wu@umist.ac.uk

ABSTRACT: A Microstrip-Coupled Rectangular Dielectric Resonator Antenna (RDRA) operated at the dominant TE^{y}_{111} mode of operation is investigated numerically and experimentally. The effect of resonator displacement along the feed line on the radiation performance of the RDRA is studied. The antenna structure is simulated using the High Frequency Structure Simulator (HFSS) software package. A few experimental set-ups were also examined and the antenna parameters were measured. The simulated results are presented and compared with those obtained by experiments. It is shown that the position of the resonator could significantly affect the radiation properties of the RDRA and there are good agreements between numerical and experimental results.

Keywords: Dielectric Resonator, Antennas and Finite Element Method (FEM)

1. Introduction

Dielectric Resonators (DRs) are widely used in shielded microwave circuits such as filters and oscillators. In recent years, the study of using open DRs as antenna has grown due to offering advantages including small size, light in weight, large bandwidth, simple feed structure and high radiation efficiency over conventional types of antennas [1-6]. Dielectric resonators have been studied in literature in hemispherical, cylindrical, cylindrical ring and rectangular geometry. Compared with the other geometry's, RDRs [5, 6] have a few advantages in fabrication process, and electrically they have two independent aspect ratios, which could be chosen to provide the required radiation patterns, gain, resonance frequency, input impedance and bandwidth. DRs can be fed using different feed arrangements including coaxial probe, microstrip line, microstrip-slot and co-planner waveguide. In 1998 Kranenburg [7] reported experimentally a Cylindrical RDRA fed by a microstrip line. Also Drossos [8] investigated a microstrip-coupled CDRA numerically and experimentally.
In this paper a microstrip-coupled RDRA operating at TE^{y}_{111} mode is investigated numerically using the FEM and the results are compared with those obtained by experiments.

2. Antenna Structure

The structure of the RDRA under investigation is shown in Figure 1. The resonator is placed directly on the top of an open-ended microstrip line. The dielectric resonator with dimensions a=19 mm, b=19 mm and h=9.5 mm is used and the relative dielectric constant of the material is ε_r=38 and g is the gap between feed line and DR. The microstrip line is etched on the topside of a piece of RT/ Duroid 5880 with dimensions 90 mm (length)×70 mm (width)×0.787 mm (thickness), dielectric constant 2.2 and copper thickness 35 μm. The feed line is 2.45mm wide giving a characteristic impedance of 50Ω [9]. The bottom side of the printed circuit board acts as a ground

plane for the microstrip line.side of the printed circuit board acts as a ground plane for the microstrip line.

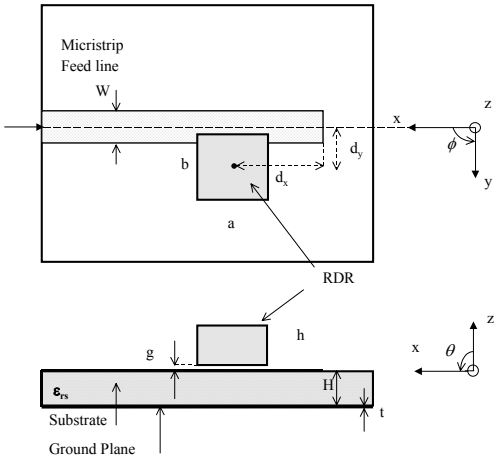

Figure 1: The microstrip-coupled RDRA structure

3. Antenna Simulation

The antenna structure is simulated using the HP85180A High Frequency Structure Simulator (HFSS), which is a software package to calculate S-parameters of the high frequency structures. The simulation technique, based on the FEM, calculates the full 3-D electromagnetic fields inside and outside (far field) of the structure. In general, in the HFSS the geometric model is automatically divided into a large number of elements, called thetrahedra, and all these elements together are refereed to as the finite element mesh. The fields in each element are represented by a local function. The value of a vector field quantity, E- or H-field, at a point inside the element is obtained using interpolation based on the value at the vertices of the each element.

Antenna structures can be analyzed using the HFSS by defining a surface, which totally surrounds the structure as an absorber boundary. This surface represents as an open space and is allowed to radiate the waves instead of being contained within. On the radiation surface, the second order radiation boundary condition is employed [10]. The radiation surface does not have to be spherical, the only restriction regarding to its shape is that they have to be convex with regard to the radiation source and to ensure accurate results, it should be applied at least a quarter of wavelength away from the source of the signal. The HFSS maps the E-field on the absorber surface and then calculates the radiation fields.

The unloaded Q-factor of the RDRA, Q_0 can be calculated from the reflection response S_{11} against frequency using one-port measurement technique presented by Wu [11]. In particular Q_0 can be expressed as $Q_\tau = \tau Q_\tau$, where Q_τ is the Q-factor at a selected reflection level $S_{11}(f_\tau)$ at f given by

$$Q_\tau = \frac{f_0}{2|f_0 - f_\tau|} \qquad 1$$

where f_0 is the resonance frequency. The parameter τ is a constant depending on the selected reflection given by:

$$\tau = \left[\frac{(1+\beta)^2 |S_{11}(f_\tau)|^2 - (1-\beta)^2}{1 - |S_{11}(f_\tau)|^2} \right]^{1/2} \qquad 2$$

where β is the coupling coefficient given by:

$$\beta = \frac{1 \mp |S_{11}(f_0)|}{1 \pm |S_{11}(f_0)|} \qquad 3$$

4. Numerical Results

The effect of the resonator position on the feed line is studied first. The variations of the resonance frequency and reflection coefficient against d_x when the resonator is symmetrically placed about x-axis (d_y=0) are shown in Figure 2a. It can be seen that two critical coupling positions are obtained. The first one is at d_x=28 mm with the resonance frequency of 2.402 GHz at which S_{11}=-39.881 dB, λ_g=91.432 mm and so d_x=0.31λ_g, where λ_g is the guide wavelength in the microstrip line at the resonance frequency. The second position is at d_x=41.5 mm with the resonance frequency of 2.162 GHz at which S_{11}=-30.392 dB, λ_g=101.727 mm or d_x=0.41λ_g.

It can also be seen that the resonance frequency decreases with increase in d_x. Figure 2b shows the variations of resonance frequency and reflection coefficient versus d_y for d_x=0.41λ_g. The resonance frequency changes slightly with d_y. The matching condition of reflection coefficient may be improved when $d_y \neq 0$. However, this happens at some specific values of d_y, e.g. d_y=1 mm.

The simulated radiation patterns of the RDRA are shown in Figures 3a and 3b for different values of d_x and d_y. It can observed that the patterns for

$d_x=0.41\lambda_g$, $d_y=0$ and $d_x=0.3\lambda_g$, $d_y=0$ are not very different from each other. Only the E-Plane pattern for $d_x=0.41\lambda_g$, $d_y=0$ is slightly wider leading to a lower directivity. On the other hand, the E-plane patterns of the RDRA positioned at $d_y=5$ mm and $d_x=0.3\lambda_g$ or $d_x=0.41\lambda_g$ are slightly deformed. This is due to unsymmetrical excitation of the resonator by the feed line.

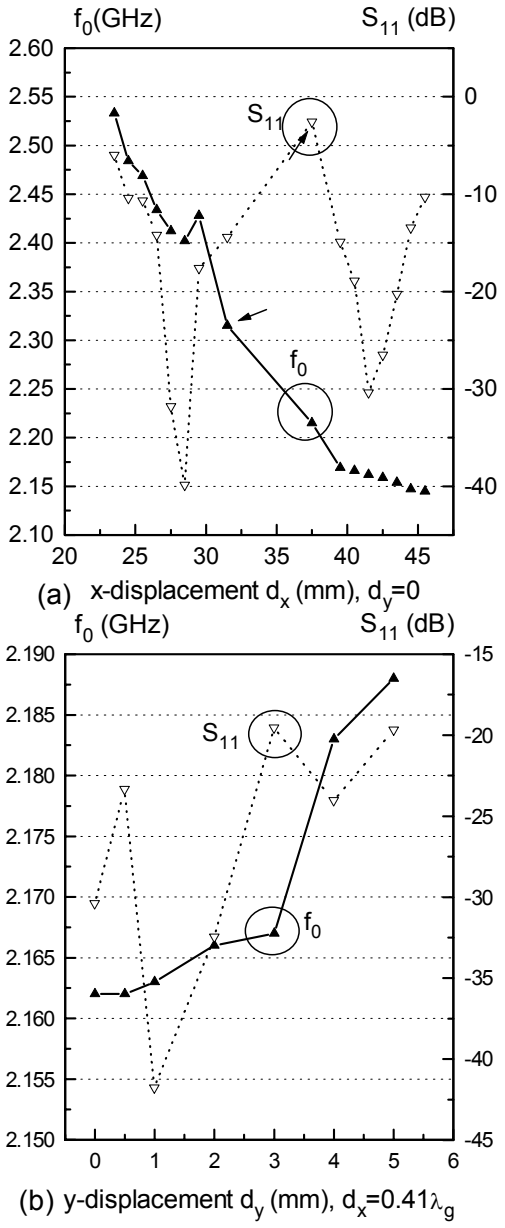

Figure 2: The measured and simulated coupling coefficient of the microstrip-coupled RDRA versus: (a) x-displacement, (b) y-displacement. (Data points: measured value, graphs: simulated results).

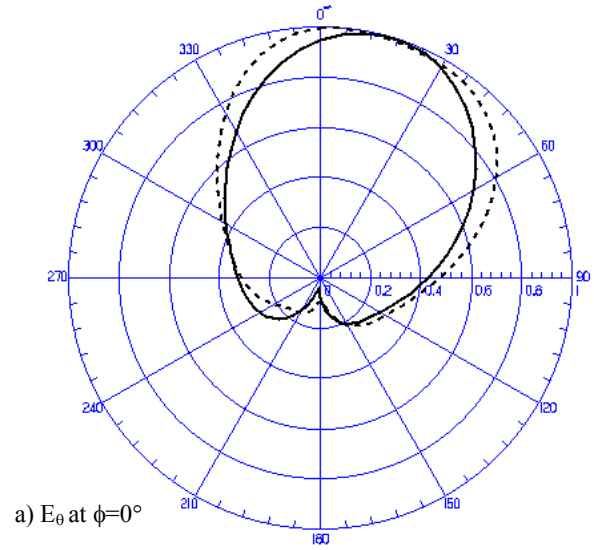

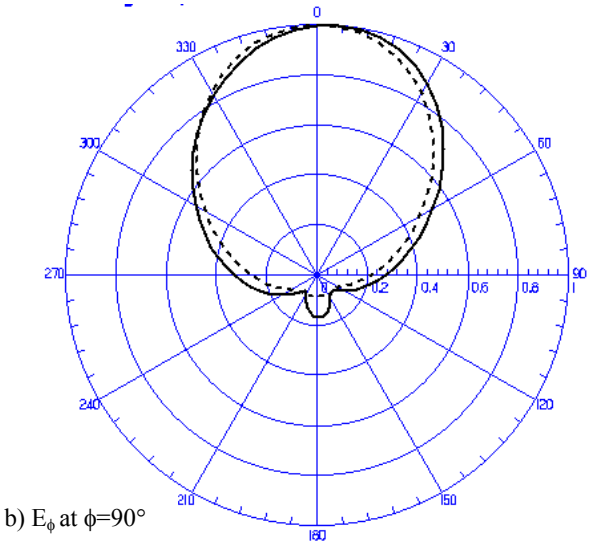

Figure 3: The simulated co-polarization radiation patterns of the microstrip-coupled RDRA at $d_x=0.31\lambda_g$, $d_y=0$ and $d_y=1$ mm and g=0: (a) E_θ at $\phi=0°$, ——— (b) E_ϕ at $\phi=90°$ ($d_x=0.31\lambda_g$, $d_y=0$, $d_x=0.31\lambda_g$,$d_y=1$ mm - - - - -).

5. Experimental Results

In order to verify the simulated results, a microstrip-coupled RDRA was implemented for measurement. A resonator with the same dimensions as used in simulation was placed on the top of an open circuited microstrip line as discussed before. The measured values of resonance frequency and reflection coefficient for different positions of the resonator along x-axis for $d_y=0$ are shown in Figures 4a and 4b. It can be

seen that antenna is matched at two positions of the DR along x-axis. For the first one, the resonance frequency is 2.531GHz and $|S_{11}(f_{01})|$=-34.9dB, corresponding to d_x=27.5mm from the open end which is at $d_x=0.31\lambda_g$. The second best match position is at d_x=46.5mm, f_0=2.326GHz and $|S_{11}(f_{02})|$=-43.9dB corresponding to $d_x=0.49\lambda_g$. These values of the x-displacement agree well with the simulated ones, i.e. ($d_x=0.31\lambda_g$, d_y=0) and ($d_x=0.41\lambda_g$, d_y=0). The displacement along y-axis was also examined for $d_x=0.49\lambda_g$ and results are shown in b. It can be seen that the maximum coupling is achieved at d_y=0, i.e. the RDRA is placed symmetrically on the microstrip line with respect to the x-axis.

The measured co-polarization radiation patterns of the RDRA versus x and y-displacement are shown in Figures 5 and 6. All other parameters of the antenna including simulation and experiments together with the results obtained by theoretical modeling using Conventional Dielectric Waveguide Model (CDWM) presented in [12] are summarized in Table 1.

6. Discussion

The simulation results show that by varying the position of the RDRA symmetrically on feed line strong coupling can be obtained at two positions on the microstrip feed line corresponding to inductive and capacitive coupling. Theoretically, the best coupling between the resonator and feed line takes place at the position of a maximum of magnetic field (inductive coupling) or a maximum of electric field (capacitive coupling) which occur at $d_x=\lambda_g/4$ and $d_x=\lambda_g/2$ from the end of the line respectively. The measured results show that the coupling coefficient agrees well with the theoretical values and also numerical ones especially in case of inductive coupling.

The measured values of resonance frequency are higher than that obtained from simulation. The error may reach ~7% in case of zero air gap (g=0). In case of capacitive coupling, the errors in prediction of Q-factor and bandwidth are 20% and 16.8% respectively as shown in Table 1. It is said that these errors [8, 12] are mainly due to the air gap between the resonator and feed line.

Moreover, it is shown that considering an air gap between the resonator and feed line in numerical procedure, the accuracy of the resonance frequency, Q-factor and input impedance bandwidth is highly improved [13].

The numerical results for radiation patterns agree well with experiments. However, they are slightly asymmetrical, especially in case of inductive coupling. This is due to the non-uniform excitation causing from the variation of fields along the length of the resonator. The measured radiation efficiency of the microstrip-coupled RDRA is also high, with a value of 91%.

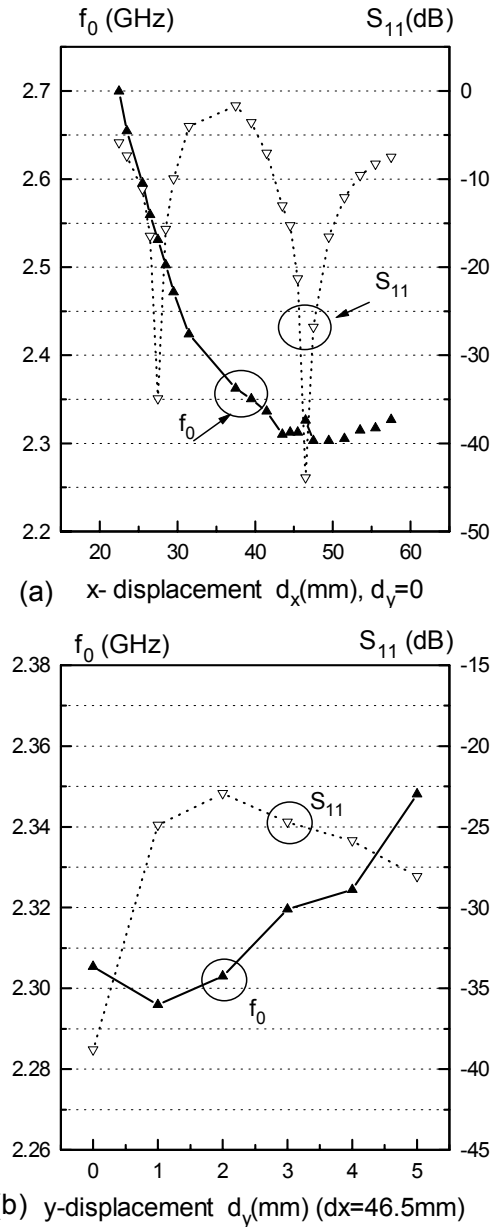

Figure 4: The measured resonance frequency and reflection coefficient of the RDRA versus: (a) x-displacement, (b) y-displacement.

7. Conclusion

In this paper a microstrip-coupled Rectangular Dielectric Resonator Antenna was studied numerically and experimentally. The HFSS software package was used to analyze the antenna by the FEM and the effect of resonator position on the feed line were studied on the radiation performance of the RDRA. A few set-ups were implemented for measurements. The results for antenna parameters were presented. Results show a good agreement between simulation and experimental results. However, better agreement could be obtained by considering the fabrication imperfection such as air gap between resonator and feed line that is needed to be taken into consideration in numerical modeling to produce more accurate prediction of antenna parameters.

8. References:

[1] McAllister, M. W., Long, S.A. and Conway, G.L., "Rectangular Dielectric Resonator Antenna", Electron. Lett. , 1998, 19, pp. 218-219.

[2] Kajfez D. & Guillon P., "Dielectric Resonators", Artech House, Norwood, MA, 1986.

[3] Mongia, R. K., "Theoretical and Experimental Resonance Frequencies of Rectangular Dielectric Resonators ", IEE Proceedings-H, 1992, 139, pp. 98-104.

[4] Mongia, R. K. and Bharita, "Dielectric Resonator Antenna- A Review & general Design Relations to Resonant Frequency and Bandwidth", International Journal of Microwave & Millimeter-Wave Computer Aided Engineering, Vol. 4, 1994, pp. 230-247.

[5] Mongia, R. K. and Ittipiboon, A., "Theoretical and Experimental Investigations on Rectangular Dielectric Resonator Antennas ", IEEE Trans., 1997, AP-45, 1997, pp. 1348-1356.

[6] Neshati M. H. and Wu, Z., "Probe-Fed Rectangular Dielectric Resonator Antennas: Theoretical Modeling & Experiments." , 10th Iranian Conference on Electrical Engineering, May 14-16, 2002, Tabriz University, Tabriz, Iran, Communication Proceedings Vol. 2 pp. 573-579.

[7] Kranenburg R. A. and Long S. A., "Microstrip Transmission Line Excitation of Dielectric Resonator Antennas", Electronics Letters, 1998, Vol. 24, pp. 1156-1157.

[8] Drossos G., Wu Z. and Davis L. E., "Theoretical and Experimental Investigations on a Microstrip-coupled Cylindrical Dielectric Resonator Antenna", Microwave & Optical Technology Letters, 1999, Vol. 21, pp.18-25.

[9] Edwards T., "Foundation for Microstrip Circuit Design. ", 1992, John Wiley & Sons.

[10] Hewlett-Packard, "HP85180A High Frequency Structure Simulator. User's Reference", 1994.

[11] Wu Z., and Davis L. E., "Automation-Oriented Techniques for Quality-Factor Measurement of high T_c Super conducting Resonators", IEE Proceedings of Science, Measurement & Technology", 1994, Vol.141, pp. 427-430.

[12] Neshati M. H. and Wu, Z., "Probe-fed Rectangular Dielectric Resonator Antennas: Theoretical Modeling & Experiments", International Journal of Engineering (IJE), Vol. 16, No. 1, Feb. 2003, pp. 41-46., Tehran, Iran.

[13] **Neshati M. H., "Numerical Modeling & Application Studies of Rectangular Dielectric Resonator Antennas", PhD Dissertation, UMIST (University of Manchester Institute of Science & Technology), Manchester, UK., 2001.**

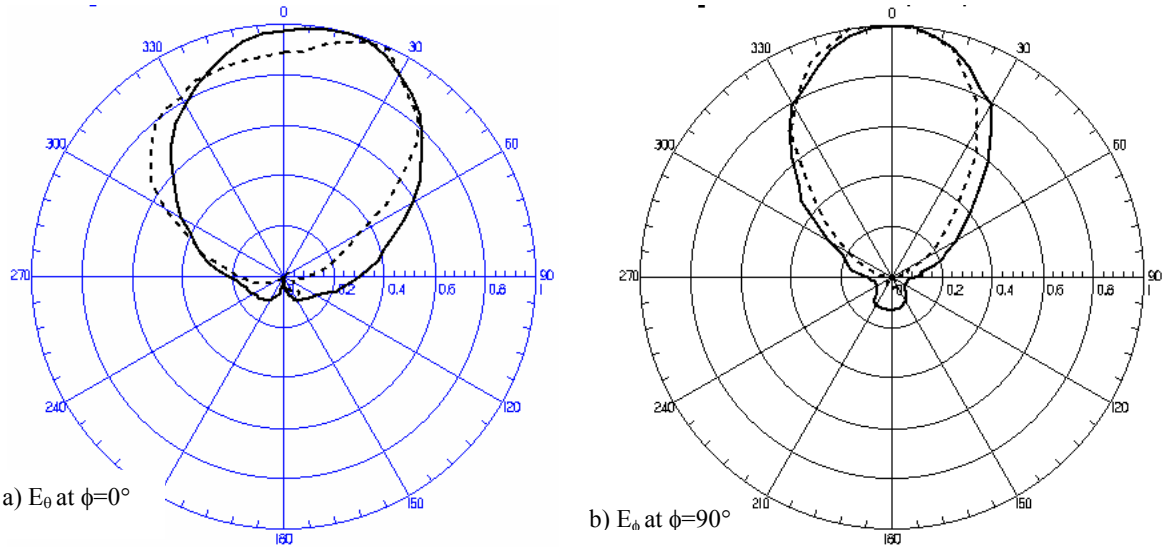

a) E_θ at ϕ=0° b) E_ϕ at ϕ=90°

Figure 5: The measured co-polarisation radiation patterns of the RDRA for different displacement :a) E_θ at ϕ=0°, b) E_ϕ at ϕ=90°d_x=0.31λ_g ,d_y=0 ——— ,d_x=0.31λ_g ,d_y=1mm - - - - -

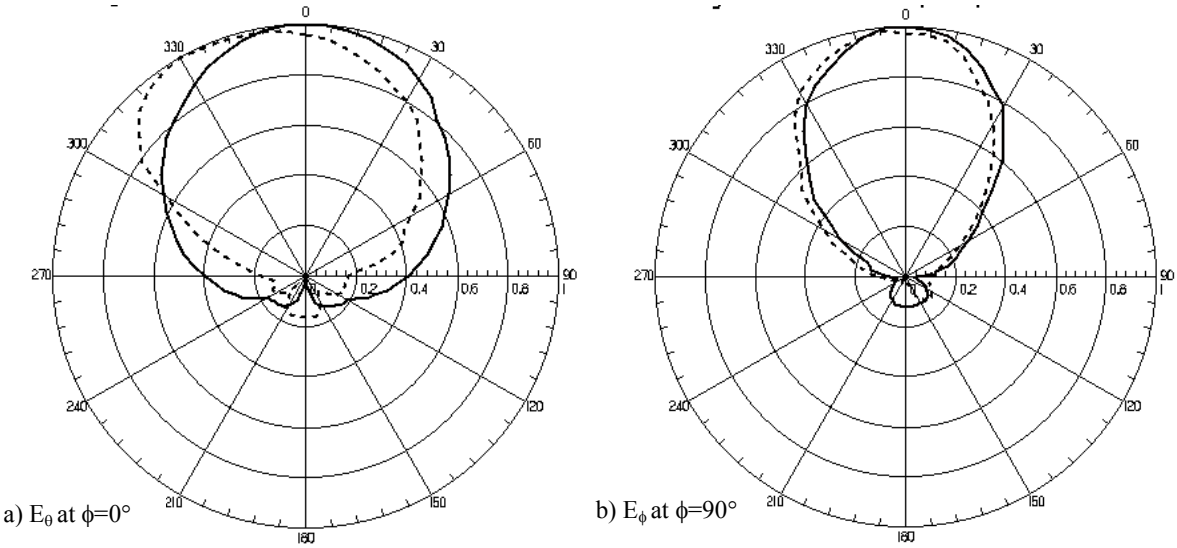

a) E_θ at ϕ=0° b) E_ϕ at ϕ=90°

Figure 6: The measured co-polarization radiation patterns of the RDRA for different displacement :a) E_θ at ϕ=0°, b) E_ϕ at ϕ=90°, d_x=0.49λ_g ,d_y=0 ,——— d_x=0.49λ_g ,d_y=1mm - - - -

Table 1: The theoretical, simulated and measured results of the microstrip-coupled RDRA at match points and their difference (%) with respect to measurement

RDRA Position	**Measured** **Theory** **Simulation**	**$d_x=0.32\lambda_g$, $d_y=0$** **$d_x=0.25\lambda_g$, $d_y=0$** **$d_x=0.31\lambda_g$, $d_y=0$**	**$d_x=0.49\lambda_g$, $d_y=0$** **$d_x=0.5\lambda_g$, $d_y=0$** **$d_x=0.41\lambda_g$, $d_y=0$**
f_0 (GHz)	Measured Theory (CDWM) Simulation	2.531 2.022 (-20.1%) 2.402 (-5.0%)	2.326 2.022 (-13%) 2.162 (-7.0%)
S_{11} (dB)	Measured Theory Simulation	-34.912 - -28.613 (18.0%)	-49.305 - -38.668 (21.6%)
β	Measured Theory Simulation	1.037 - 1.053 (1.5%)	0.987 - 0.941 (-4.6%)
Directivity, Gain	Measured Theory Simulation	3.205 2.880 (-10.1%) 4.700 (46.6%)	3.023 2.880 (-4.7%) 4.218 (36.5%)
Q-factor	Measured Theory Simulation	26.287 33.088 (25.8%) 36.617 (39.3%)	30.028 33.088 (10.2%) 36.052 (20%)
BW (%) VSWR≤2.6	Measured Theory Simulation	3.8 3.02 (-20%) 2.73 (28%)	3.33 3.02 (-9%) 2.77 (-27.2%)
Radiation Efficiency (%)	Measured Theory Simulation	90.5 100 (9.5%) -	90.5 100 (9.5%) -